

Axon Morphology Analysis: From Image Processing to Modelling

Alejandro Mottini

Advisor: Xavier Descombes (INRIA)

Collaborator: Florence Besse (IBV)

Prepared at Morpheme Team (INRIA/IBV/I3S)



Institut Valrose
Biologie



Outline

- 1 Introduction
- 2 Axon Extraction from Fluorescent Confocal Microscopy Images
- 3 Distance Between Trees Using the Elastic Shape Analysis Framework
- 4 Discrete Stochastic Model for the Generation of Axonal Trees
- 5 Conclusions

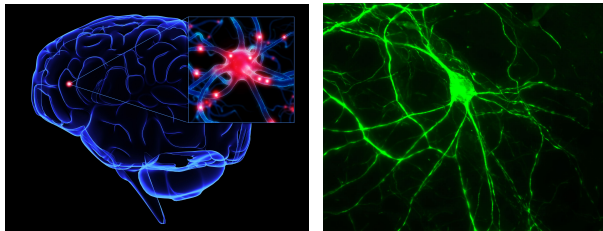
Outline

- 1 Introduction
- 2 Axon Extraction from Fluorescent Confocal Microscopy Images
- 3 Distance Between Trees Using the Elastic Shape Analysis Framework
- 4 Discrete Stochastic Model for the Generation of Axonal Trees
- 5 Conclusions

[Introduction](#)[Biological Context](#)

Biological Context

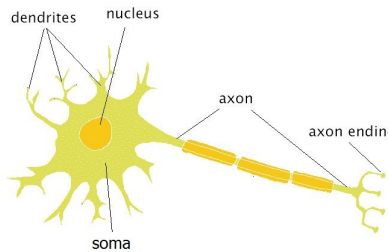
- The brain is the most complex biological organ, both in terms of structure and functioning
- It is composed of billions of neurons that interconnect to form neural circuits
- They are essential to the processing and storage of information



[Introduction](#)[Biological Context](#)

Biological Context

- Neurons communicate with one another through synapses using 2 types of protrusions: dendrites and axons
- Axons are long tree like structures that transmit information to neighboring cells
- Only one axon per neuron

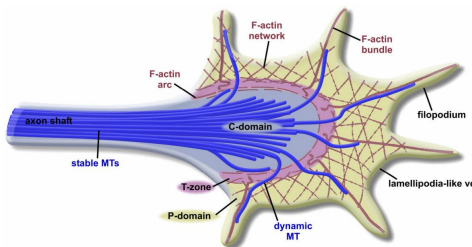


Introduction

Biological Context

Biological Context

- During the development of the nervous system, neurons extend their axons to form neural circuits
- Axons are guided to their target by their growth cone (GC)
- GC sense chemical signals present in their environment
- The paths taken by the GC depend on these signals (can be attractive or repulsive)

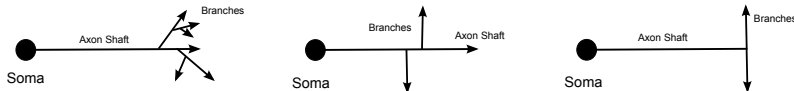


Introduction

Biological Context

Biological Context

- Once an axon reaches its destination, it stops
- Branch generation process then begins
- Branches will connect the neuron to multiple targets (neighboring cells)
- Different branching configurations adapted to different connection requirements



[Introduction](#)[Motivation](#)

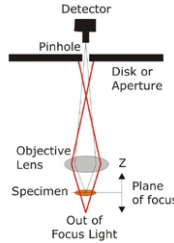
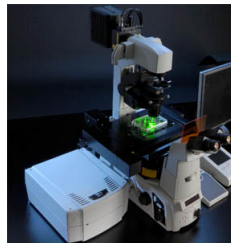
Motivation

- Morphological characteristics are linked to the neuron ability to function properly
- I.e: number of branches in an axon is related to the number of connections the neuron can make
- These characteristics are also able to characterize pathological states
- I.e: Fragile X Syndrome is related to unusual morphological characteristics of the axons
- The morphological analysis of axons is of great importance

[Introduction](#)[Motivation](#)

Motivation

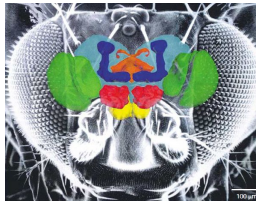
- Axon morphology is analyzed using confocal microscopy images
- This technique offers several advantages over conventional optical microscopy
- Is capable of obtaining sharp 3D images of thick specimens



[Introduction](#)[Motivation](#)

Motivation

- Collaboration between computer scientists (INRIA/I3S) and biologists (IBV)
- Image database of axons from *Drosophila*
- Both wild (normal) and mutant (pathological) neurons have been considered
- Mutant neurons were obtained by inactivating certain genes related to neurological diseases in humans
- Used to validate the different algorithms



[Introduction](#)[Motivation](#)

Motivation

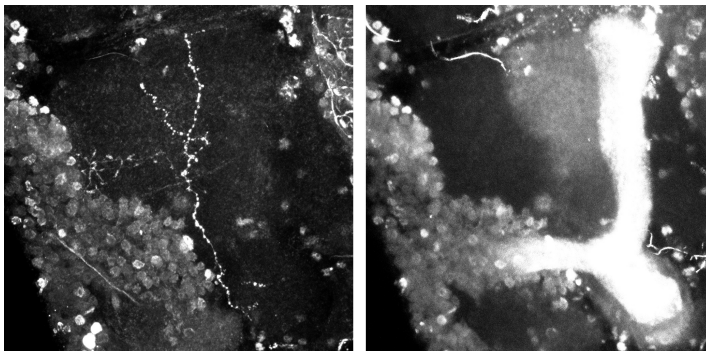
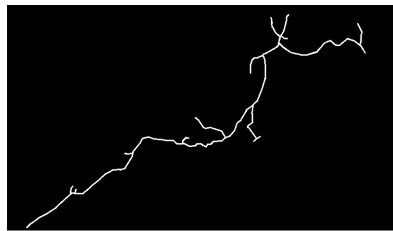
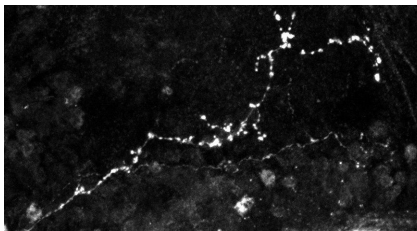


Figure: Channel 1 (left; GFP staining) and 2 (right; Fasciclin II staining) for a given image (maximum intensity projections).

Objectives

- Images need to be processed to extract the information
- First necessary step is segmentation
- We propose a new algorithm adapted to our images



Objectives

- After extraction, quantification of differences between populations
- We propose
 - A new approach based on the Elastic Shape Analysis Framework
 - A method for the computation of the average shape of a population
- We use them to analyze, compare and classify populations of axons

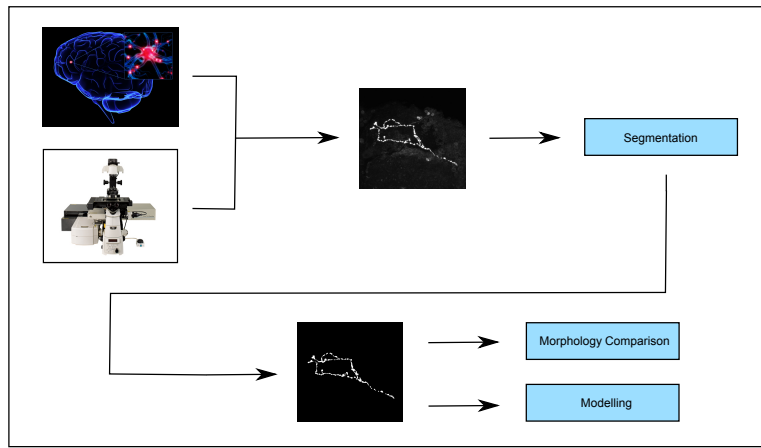
Objectives

- A different approach to morphological analysis: modelling
- We propose a new discrete stochastic model for the generation of axonal trees
- Parameters provide another tool to characterize and classify the populations.

Introduction

Objectives

Objectives



Outline

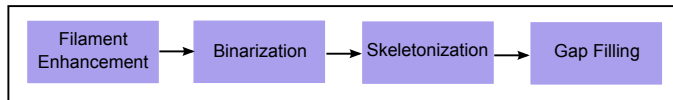
- 1 Introduction
- 2 Axon Extraction from Fluorescent Confocal Microscopy Images
- 3 Distance Between Trees Using the Elastic Shape Analysis Framework
- 4 Discrete Stochastic Model for the Generation of Axonal Trees
- 5 Conclusions

Axon Extraction: Introduction

- Key problem in the field of neuron image analysis (DIADEM Challenge)
- Very challenging problem
- Most common segmentation approach is semi automatic tracing (difficult and time consuming)
- Many available methods, each one adapted to different situations:
 - Neuromatic (manual)
 - V3D-Neuron (semi automatic, graph-based algorithm)
 - NeuronStudio (semi automatic, multi-step approach)
 - Zhang et al. (semi automatic, designed for images of multiple non branching axons)
 - Tree2Tree (automatic, multi-step approach, 2D)

Introduction

- Requirements:
 - In vivo data (noisy, spurious information)
 - 3D datasets
 - Automatic extraction
 - Easy to use
- None of the reviewed methods obtained satisfactory results
- A new multi-step segmentation method is proposed
- Combines algorithms for filament enhancement, binarization, skeletonization and gap filling
- Capable of extracting axons from confocal microscopy images
- We do not consider the more challenging case of multiple axons per image



Axon Extraction: Filament Enhancement

- Different approaches exist in the literature (i.e: Frangi et al., Wilkinson et al.)
- We propose a multiscale filter based on Gabor functions
- We process each 2D slice independently (non isotropic resolution)
- The analysis could be extended to 3D in the future

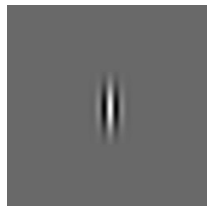
Filament Enhancement

- Classical Gabor functions are defined as:

$$G(x, y) = \cos\left(\frac{x_1\pi}{\sqrt{2}\lambda}\right) \exp\left(-\frac{x_1^2 + \gamma^2 y_1^2}{2\sigma_g^2}\right)$$

- Where $x_1 = x \cos(\theta) + y \sin(\theta)$ and $y_1 = x \sin(\theta) - y \cos(\theta)$
- Parameters $\theta, \lambda, \sigma_g, \gamma$ control the orientation, wavelength, etc
- Given an image $I(x, y)$, the filtered image H is defined as:

$$H = \|G * I\|$$



Filament Enhancement

- Based on the previous G filter, we propose some modifications
- To avoid false positives on edges, two filters are considered (left and right):

$$G^+(x, y) = \begin{cases} \cos\left(\frac{x_1\pi}{\sqrt{2}\lambda}\right) \exp\left(-\frac{x_1^2 + \gamma^2 y_1^2}{2\sigma_g^2}\right) & \text{if } x_1 \geq 0 \\ 0 & \text{otherwise} \end{cases}$$

$$G^-(x, y) = \begin{cases} \cos\left(\frac{x_1\pi}{\sqrt{2}\lambda}\right) \exp\left(-\frac{x_1^2 + \gamma^2 y_1^2}{2\sigma_g^2}\right) & \text{if } x_1 < 0 \\ 0 & \text{otherwise} \end{cases}$$

Filament Enhancement

- We define:

$$\begin{aligned}\Psi^{-,+}(x, y) = & \eta_-^{-,+} G^{-,+}(x, y) \delta(G^{-,+}(x, y) < 0) + \\ & + \eta_+^{-,+} G^{-,+}(x, y) \delta(G^{-,+}(x, y) \geq 0)\end{aligned}$$

- Constants $\eta_-^-, \eta_-^+, \eta_+^-$ and η_+^+ are obtained by normalizing the filters:

$$\begin{cases} \int_{\mathbb{R}^2} \Psi^{-,+}(x, y) dx dy = 0 \\ \int_{\mathbb{R}^2} \max(0, \Psi^{-,+}(x, y)) dx dy = 1 \end{cases}$$

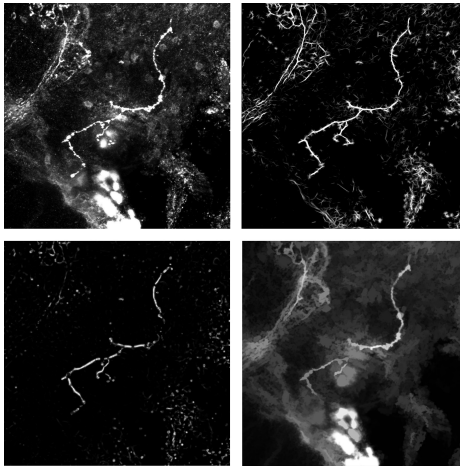
- This eliminates their dependency to the absolute intensity of the image
- Finally, the filament enhancement filter is given by:

$$F = \min(\|\Psi^- * I\|, \|\Psi^+ * I\|)$$

Filament Enhancement

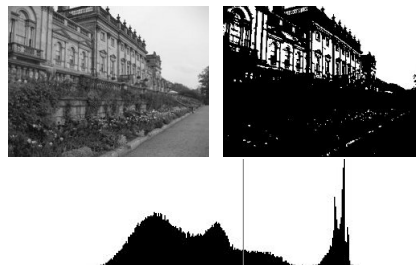
- Multiscale analysis: width of filter is varied between the expected axon widths (σ_g)
- θ is varied to test for filaments in all directions
- Remaining parameters are set by imposing certain conditions (i.e filter value equal to 0 at the edge of the filament)
- Filter evaluated against 2 other filament enhancement filters (*Frangi et al.* and *Wilkinson et al.*)

Filament Enhancement



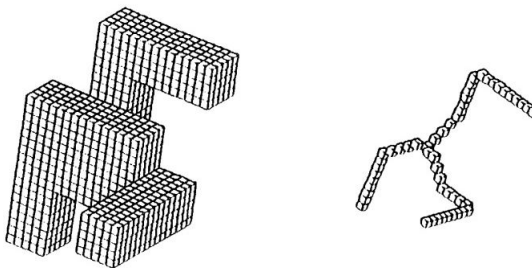
Axon Extraction: Binarization

- Binarization of the filtered images based on Otsu's thresholding
- Finds the threshold maximizing the between-class variance
- Algorithm makes several assumptions (i.e. image presents a bimodal histogram)



Skeletonization

- Binary image is then skeletonized
- Skeleton is used as a way of summarizing the geometrical and topological properties of the shape
- It loses the width information that is not relevant for our application
- We use the implementation proposed by *R. Van Uitert et al.* that preserves topology



Gap Filling

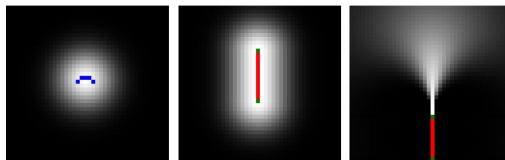
- Extracted skeleton can present discontinuities (gaps) due to the binarization in a noisy context
- We use tensor voting approach for filling them in 3D (*Risser et al.*)
- Algorithm is divided into 4 steps:
 - Tokenization
 - Creation of tensor field T
 - Creation of saliency map
 - Reconnection

Gap Filling - Tensor Field Creation

- Assigns to each token a local tensor field
- We consider the contributions of all the tokens in the image by adding the local fields:

$$T(i, j, k) = \sum_{n=1}^N TE_n(i, j, k) + \sum_{m=1}^M TI_m(i, j, k) + \sum_{q=1}^Q TS_q(i, j, k)$$

- Contributions depends on the type and properties of each token

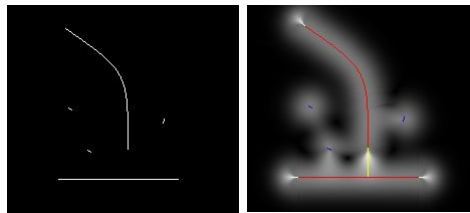


Gap Filling - Saliency Map Creation

- Consists in generating a scalar field
- For each voxel, the value of the field equals:

$$S(i, j, k) = \lambda_1(i, j, k) - \lambda_2(i, j, k)$$

- Where $\lambda_{1,2}(i, j, k)$ are the two biggest eigenvalues (absolute value) of tensor field T in the point (i, j, k)



- The algorithm reconnects the paths along the points with maximum saliency
- The largest CC corresponds to the axon

Step by Step

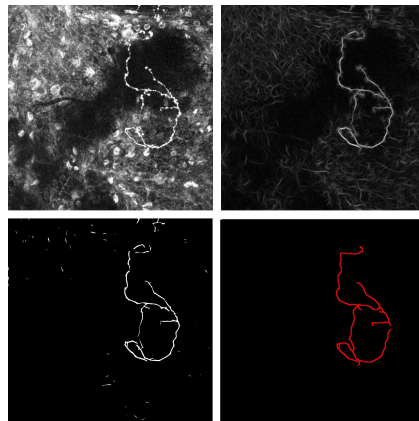


Figure: Results obtained on each step of the algorithm. Top: original image (left) and filament enhancement (right). Bottom: binarization (left) and final result (right) (maximum intensity projections).

Validation

- Validated on a subset of the IBV image database
- 12 3D images with different noise levels and tree complexities were considered
- Both normal and mutant axons were considered
- Manual segmentations were compared with our method, V3D and NeuronStudio
- 3 quantitative measures were used for the evaluation:
 - Hausdorff Distance (Hausdorff) (the lower the value the better)
 - Root Mean Square Error (RMSE) (the lower the value the better)
 - Patt's Figure of Merit (FOM) (the bigger the value the better)

Results

Method	FOM (Mean/Std)	Hausdorff (Mean/Std)	RMSE (Mean/Std)
PM	0.34 / 0.08	154.18 / 79.19	2.83 / 0.54
V3D	0.09 / 0.03	145.97 / 107.29	4.73 / 1.2
NeuronStudio	0.01 / 0.04	182.71 / 91.35	9.1 / 1.11

Table: Quantitative comparison between the proposed method (PM), V3D and NeuronStudio with the manual segmentation (mean and std)

- For the FOM and RMSE criteria, our method outperforms V3D and NeuronStudio in all the images
- Hausdorff criterion shows a more balanced performance:
 - Our method outperforms V3D in very noisy images
 - If axonal tree is clearly visible, V3D obtains better results
 - NeuronStudio is outperformed by the two other methods in all images except one

Results

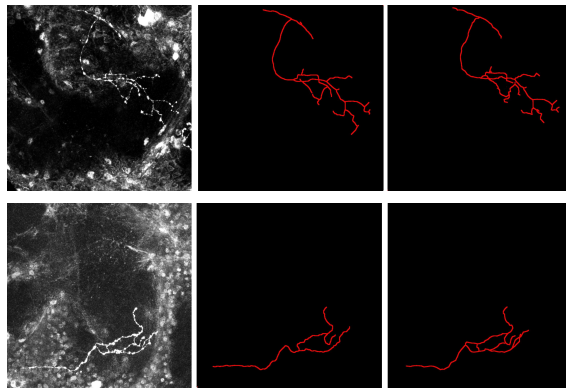


Figure: Comparison between original image (left), our result (middle) and ground truth (right) (maximum intensity projections).

Results

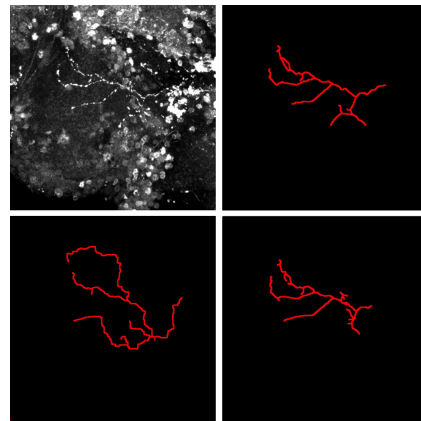


Figure: Comparison between original image (top left), the ground truth (top right), V3D (bottom left) and our result (bottom right) (maximum intensity projections).

Results

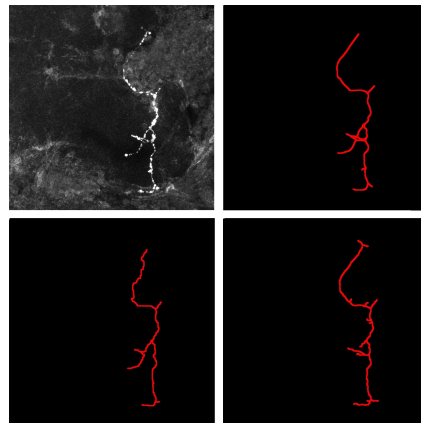


Figure: Comparison between original image (top left), the ground truth (top right), V3D (bottom left) and our result (bottom right) (maximum intensity projections).

Summary

- Algorithm for the automatic extraction of axons from fluorescent confocal microscopy images
- Relies on several steps: filament enhancement, binarization, skeletonization and gap filling
- Tested on 12 3D images of the IBV database, compared with ground truth and 2 other methods
- Outperforms the other algorithms in most cases
- **Limitations:**
 - Can connect filaments that should not be connected (alters morphology)
 - Manual setting of some parameters

Outline

- 1 Introduction
- 2 Axon Extraction from Fluorescent Confocal Microscopy Images
- 3 Distance Between Trees Using the Elastic Shape Analysis Framework
- 4 Discrete Stochastic Model for the Generation of Axonal Trees
- 5 Conclusions

Introduction

- Comparison and classification of neuronal morphologies is an important problem in neuroscience
- Can be used to study the functional properties of populations or to evaluate segmentation algorithms
- Different approaches in the literature:
 - DIADEM metric (topological)
 - Feragen et al. (topological and geometrical)
 - TED (tree-edit distance, purely topological)
 - Path2Path (topological and geometrical)
 - Feature Based Classification

Introduction

- We propose a new distance that considers topological and geometrical information
- Based on the Elastic Shape Analysis Framework (ESA)
- Mathematical framework for the comparison of curves in R^3
- Working in the space of curves, geodesics and distances can be found between them (points in the manifold)

Elastic Shape Analysis Framework

- Starting point: curves in R^3 : $\beta : [0, 1] \rightarrow R^3$
- Curves are reparameterized in a special way (squared root velocity function):

$$q(t) = \frac{\dot{\beta}(t)}{\sqrt{\|\dot{\beta}(t)\|}}$$

- The set of all the SRVF parameterized curves in R^3 defines a manifold (the preshape space):

$$C = \{q : [0, 1] \rightarrow R^3\}$$

- Different versions of the same curve (rotated, etc) have different images in C (different q)

Elastic Shape Analysis Framework

- Shape preserving transformations (translation, scale, rotation and reparametrization) are removed (to only compare shapes)
- Elements in C that represent the same shape can be unified:

$$[q] = \{O(q \circ \gamma) \sqrt{\dot{\gamma}} | O \in SO(n), \gamma \in \Gamma\}$$

- Where $SO(3)$ is the group of 3×3 rotation matrices and Γ the group of all reparameterizations
- Each class $[q]$ defines an unique shape
- Set of all equivalence classes is the shape space S (quotient space of C)
- The framework allows us to compute geodesics between points in S
- Each geodesic path is viewed as an elastic deformation of one shape into the other, and its length the distance between the two curves

Elastic Shape Analysis Framework

- Distance between two curves:

$$d(\beta_1, \beta_2) = \min_{\gamma \in \Gamma, O \in SO(3)} \|q_1 - O(q_2, \gamma)\|, \text{ with } \gamma \in \Gamma, O \in SO(3)$$

- Let γ^* and O^* be the reparametrization and the rotation that minimize the distance (found using dynamic programming and SVD)
- Geodesic path between the 2 curves is given by:

$$\alpha(\tau) = (1 - \tau)q_1 + \tau(O^*(q_2, \gamma^*))$$

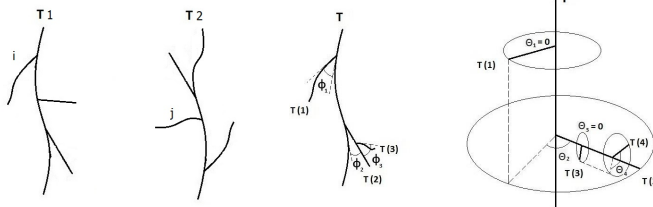
Elastic Shape Analysis Framework - β_t Function

- This framework was extended to include additional information of the curve β .
- I.e. object matching: β represents contour and β_t the locations of certain landmarks
- This information is included as an additional component of the curve

$$\beta(t) = \begin{bmatrix} \beta_s \\ b \cdot \beta_t \end{bmatrix} \in R^{3+1}$$

- $b > 0$ controls the influence of the β_t function

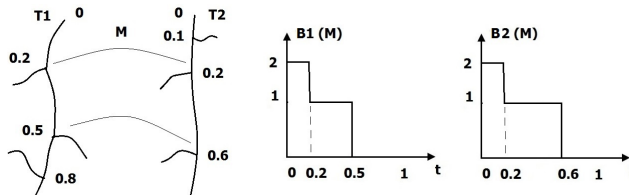
Distance Between Trees



- Extension to trees
- Let us consider T_1 and T_2
- Each one represented by 3D open curves in R^3
- We define a matching function $M : (0, 1, 2, \dots, n) \times (0, 1, \dots, m)$

Distance Between Trees

- We define a branch function $B(t)$
- For a point t , indicates how many **matched** branches remain after it (from the root)
- Provides a way to take into account the difference of position of matched branches



Distance Between Trees - Definition

- Distance between trees T_1, T_2 :

$$D_{ESA}(T_1, T_2) = \min_M [d((\beta_1(t), B_1(t, M)), (\beta_2(t), B_2(t, M))) + \\ + \sum_{(i,j)} \alpha_{i,j} M(i, j) D(T_1(i), T_2(j))]$$

- M is the matching function, $\alpha_{i,j}$ a weight parameter and $D(T_1(i), T_2(j))$ the distance between the matched branches i and j (sub trees)
- $D(T_1(i), 0) = w_{kill}$
- $D(T_1(0), T_2(0))$ represents the distance between the main axons
- Sub branches are taken into account in a recursive way in the second term

Distance Between Trees - Definition

- Distance between two matched branches:

$$\begin{aligned} D(T_1(i), T_2(j)) = & d_{length}(\beta_{T_1(i)}, \beta_{T_2(j)}) + \\ & + w_1 d_{shape}((\beta_{T_1(i)}, B_{T_1(i)}), (\beta_{T_2(j)}, B_{T_2(j)})) + \\ & + w_2 d_{angle}(\beta_{T_1(i)}, \beta_{T_2(j)}) \end{aligned}$$

- $\beta_{T_k(l)}$ is the curve corresponding to branch l of tree k , $B_{T_k(l)}$ its associated B function
- d_{length} depends on the difference in length between the two branches
- d_{shape} is found using the Elastic Shape Analysis distance
- d_{angle} depends on the angles Φ, Θ between the two branches

Distance Between Trees - Optimization

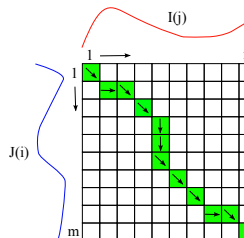
- Distance requires to find optimum matching of branches
- Express our branch matching problem as an assignment problem
 - Murty ranked assignment algorithm: global minimum but slow

Tasks		
Resources ↓	5	7
1	3	5
4	4	2

- Approximated solution using the Dynamic Time Warp framework (DTW)

Distance Between Trees - Optimization - DTW

- Widely used in speech recognition
- Measures the difference between 2 signals $I = [i_1, i_2, \dots, i_n]$ and $J = [j_1, j_2, \dots, j_m]$ by stretching and compressing them to minimize the distance between them
- Constructs a cost matrix containing pairwise distances between the signals
- Finds the optimum path $P = [p_1, p_2, \dots, p_K]$ (where $p_x = [i_q, j_r]$)



Validation - Distance

- Validated using 2 database
- IBV: 61 images (20 normal, 24 type 1 mutant and 17 type 2 mutant)
- NeuroMorpho.Org: 131 images (10 granule cell, 41 type I, 40 uniglomerular projection neuron and 40 motoneuron)
- We validate against TED, Path2Path and feature based approach (8 features)
- We embed the 3 distances in K-means to classify the populations

Validation - Distance

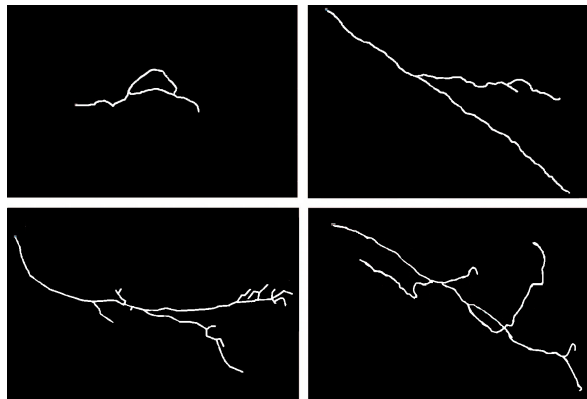


Figure: Examples of neurons from each of the four chosen populations of NeuroMorpho: Mouse granule cell (top left), Agouti type I (top right), *Drosophila* uniglomerular projection neuron (bottom left) and Mouse motoneuron (bottom right); (2D projections)

Results - NeuroMorpho

Table: Sensitivity for the granule cell (S-G), type I (S-TI), uniglomerular projection neuron (S-U) and motoneuron (S-M) populations and overall accuracy (OA) for ESA, the feature-based classification scheme (FBC), Path2Path (P2P) and RTED.

Method	S-G	S-TI	S-U	S-M	OA
ESA	100.0%	75.6%	97.5%	80.0%	85.5%
FBC	0.0%	36.6%	92.5%	47.5%	54.2%
P2P	40.0%	58.5%	75.0%	30.0%	53.4%
RTED	0.0%	63.4%	87.5%	17.5%	51.9%

- ESA distance outperforms the other methods
- Remaining methods obtain a similar overall accuracy
(Path2Path: more balanced results)

Results - IBV

Table: Sensitivity for the normal (S-Normal) and mutant (S-Mutant) populations and overall accuracy (OA) for ESA, the feature based classification scheme (FBC), Path2Path (P2P) and RTED.

Method	S-Normal	S-Mutant T_1	S-Mutant T_2	OA
ESA	85.0%	66.7%	70.6%	73.8%
FBC	90.0%	58.3%	47.1%	65.6%
P2P	70.0%	79.2%	23.5%	60.7%
RTED	47.4%	50.0%	47.1%	48.3%

- Best overall accuracy using the ESA distance
- More balanced performance of the methods

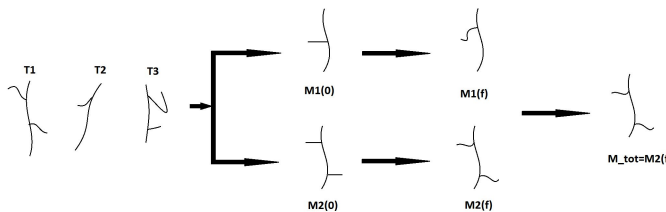
Distance Between Trees - Mean Shape

- First step necessary for the statistical analysis of a population
- Trivial when working in Euclidean spaces, several difficulties in more general manifolds
- Usually, the mean m of a set of points x_i in a space S with a metric d is defined as:

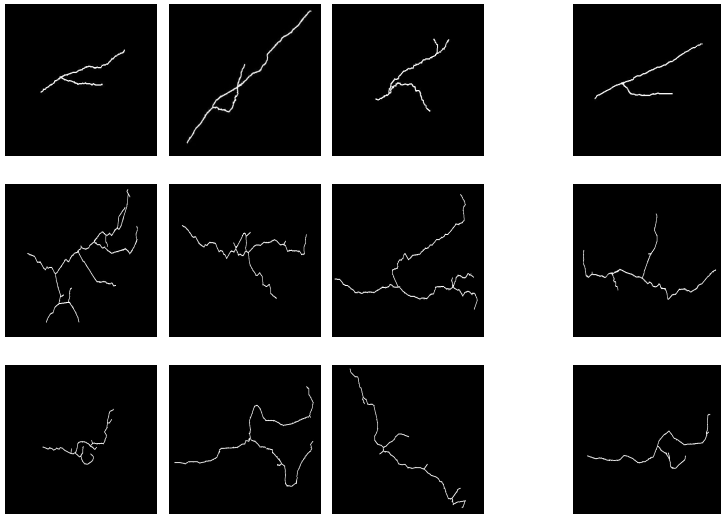
$$m = \arg \min_{x \in S} \sum_{i=1}^n d(x, x_i)^2$$

Distance Between Trees - Mean Shape

- We compute several means, each with a different number of branches
- For each we consider an iterative algorithm
- The final mean will be the one presenting the minimum average distance to its population



Distance Between Trees - Mean Shape



Validation - Mean Shape

- Validated on both databases
- We have calculated the mean trees of each population
- The mean shapes were used in a 3-fold cross validation scheme to classify the samples
- Kruskal-Wallis one-way non parametric analysis of the overall accuracy values obtained for each method

Results - NeuroMorpho



Figure: Mean shapes for the four populations taken from NeuroMorpho: granule cell (top left), type I (top right), uniglomerular projection neuron (bottom left) and motoneuron (bottom right); (2D projections).

Results - NeuroMorpho

Table: Sensitivity for the granule cell (S-G), type I (S-TI), uniglomerular projection neuron (S-U) and motoneuron (S-M) populations and overall accuracy (OA) for ESA using the mean shape (ESA WM).

Method	S-G	S-TI	S-U	S-M	OA
ESA WM	100.0%	95.1%	100.0%	95.0%	96.9%

- Obtains the best result of all the tested methods (**reminder:** ESA without mean obtained a OA of 85.5%)
- Suggest that the mean trees represent well the populations

Results - NeuroMorpho

Table: Mean, standard deviation (Std), maximum (Max) and minimum (Min) of the overall accuracy on the test sets for each method (ESA with mean, P2P and TED).

Set	Mean	Std	Max	Min
ESA	95.3%	2.8%	100.0%	84.6%
P2P	39.8%	9.2%	61.0%	23.3%
TED	22.7%	8.6%	56.6%	11.1%

- ESA produced stable results, and a higher average overall accuracy
- Kruskal-Wallis: $p = 5, 3e^{-34}$ (accuracy difference between ESA and the other methods is statistically significant)

Results - IBV

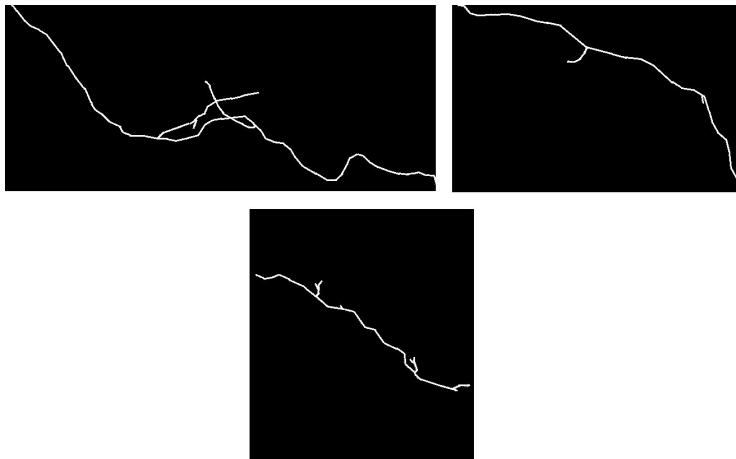


Figure: Mean normal (top left), mutant type 1 (top right) and mutant type 2 (bottom) axonal trees (2D projections).

Results - IBV

Table: Sensitivity for the normal (S-Normal) and mutant (S-Mutant) populations and overall accuracy (OA) for ESA using the mean shape (ESA WM).

Method	S-Normal	S-Mutant T_1	S-Mutant T_2	OA
ESA WM	90.0%	83.3%	70.6%	80.3%

- Results improve when using the mean shape (**reminder**: ESA without mean obtained a OA of 73.9%)

Summary

- Method for the comparison of tree-like structures
- Both geometrical and topological information is considered
- Extension of the Elastic Shape Analysis Framework
- Method for the computation of the mean shape of population
- Validated on 2 image databases (near 200 images)
- Compared against 3 methods, we obtain a better overall performance
- **Limitations:**
 - Parameters manually calibrated
 - No unicity of mean shape
 - Real metric?

Outline

- 1 Introduction
- 2 Axon Extraction from Fluorescent Confocal Microscopy Images
- 3 Distance Between Trees Using the Elastic Shape Analysis Framework
- 4 Discrete Stochastic Model for the Generation of Axonal Trees
- 5 Conclusions

Introduction

- Models can help explain the system underlying processes and make predictions about its functioning
- Different neuronal development models proposed in the literature
- Differ with respect to the processes, methodology and type of data used for the parameter estimation and the dimension considered:
 - Segev et al. (2D, chemical signals considered, parameters not estimated)
 - Kobayashi et al. (3D, chemical signals considered, parameters not estimated)
 - Koene et al. (4D, very complete, no chemical signals considered)

Objective

- Develop a model for the generation of realistic axonal trees
- Consider an external attraction field
- Estimate all parameters from static images (IBV database).
- Use the parameters to characterize the different populations

Model Description

- 2D discrete stochastic model for the simulation of axonal biogenesis
- Considers 2 main biological processes:
 - Growth process: models the elongation and shape
 - Bifurcation process: models the generation of branches
- Both processes are considered to be independent from each other

Model Description - Growth Process

- The number of points N of a filament (i.e length) is determined using a Gaussian distribution $\mathcal{N}(\mu, \sigma^2)$
- The shape is determined using a third order Markov Chain that depends on the elastic properties of the neurites and on the external attraction field (parameters of the model)

Model Description - Growth Process, Shape

- Given a point n_t on a path, n_{t+1} depends on:
 - Relative positions of n_{t-1} , n_{t-2}
 - External field in n_t , given by a vector
- Two main cases are defined (plus all the possible rotations):

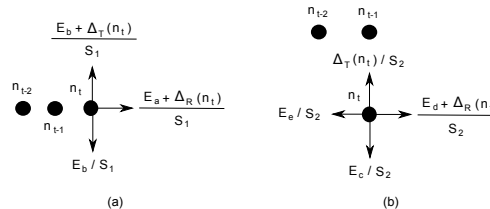


Figure: Conditional probabilities $P(n_{t+1}|n_t, n_{t-1}, n_{t-2})$

$$\begin{cases} S_1 = E_a + 2E_b + \Delta_R(n_t) + \Delta_T(n_t) \\ S_2 = E_c + E_d + E_e + \Delta_R(n_t) + \Delta_T(n_t) \end{cases}$$

Model Description - Bifurcation Process

- Bifurcation process is defined by the probability of branching P_b on each point
- $P_b(n)$ is piecewise constant during time
- Branches grow independently of the main axon following the same model.

Model Description - Parameter Estimation

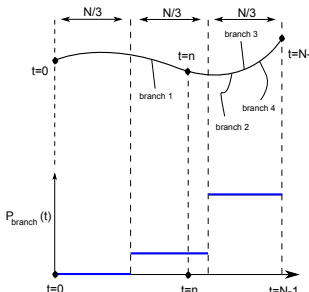
- Model parameters: $(\mu, \sigma^2, P_b, E_a, E_b, E_c, E_d, E_e)$ and the external field $(\Delta_x(u, v), \Delta_y(u, v))$, for $(u, v) \in L$.
- All estimated from real images of axonal trees

Model Description - Parameter Estimation

- Length of paths with normal distribution:

- $\hat{\mu} = \frac{\sum_{a \in A} l_a}{\text{card}(A)}$
- $\hat{\sigma}^2 = \frac{\sum_{a \in A} (l_a - \hat{\mu})^2}{\text{card}(A)}$

- Where A is a set of axonal trees and l_a , $a \in A$ the length (i.e., number of pixels) of the main branch of axon a .
- $\hat{P}_b = \frac{1}{\text{card}(A)} \sum_{a \in A} \frac{N_b(a)}{l_a}$



Model Description - Parameter Estimation

- For each configuration of the past (i.e, n_{t-1}, n_{t-2}) we obtain equations
- In total, 48 equation are considered (when we take into account all the possible rotations)
- The equations relate the remaining model parameters with the number of times the different possible configurations appear in the images

Model Description - Parameter Estimation

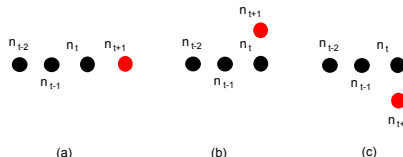


Figure: Example of possible configurations

$$\left\{ \begin{array}{l} \frac{N_1}{N_T} = \frac{\hat{E}_a + \hat{\Delta}_R}{\hat{S}_1} \\ \frac{N_2}{N_T} = \frac{\hat{E}_b + \hat{\Delta}_T}{\hat{S}_1} \\ \frac{N_3}{N_T} = \frac{\hat{E}_b}{\hat{S}_1} \\ N_T = N_1 + N_2 + N_3 \end{array} \right.$$

Where $N_{1,2,3}$ are the number of times that the configurations are present in an axon (assumption: $\hat{\Delta}_R$, $\hat{\Delta}_T$ constant)

Model Description - Parameter Estimation

- The system of 48 equations is solved with Least Mean Squared
- The parameters are estimated using sliding window scheme (to allow variation in the chain parameters)
- The optimum window size is chosen from the estimation on simulated axons:

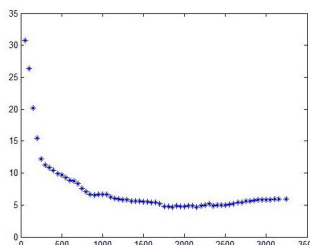
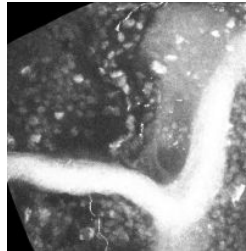
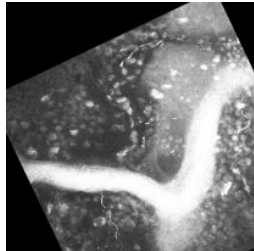
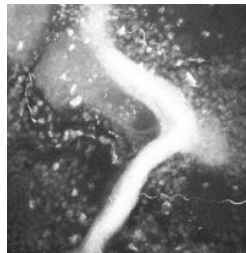
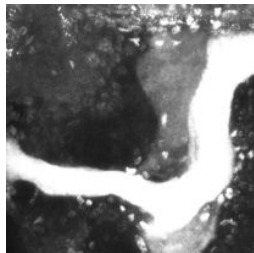


Figure: Plot of the average error between the estimated and real norm of the Δ field for different window sizes (expressed in percentage of the real norm).

Validation

- Validated on 53 images of the IBV database (subset)
- Both normal and mutated neurons were considered (18 normal, 21 type 1 mutant and 14 type 2 mutant)
- Each image has 2 channels
 - Channel 1: Axonal tree
 - Channel 2: Brain structure in which axons are developing
- Images were registered using the second channel (rigid+ non rigid)

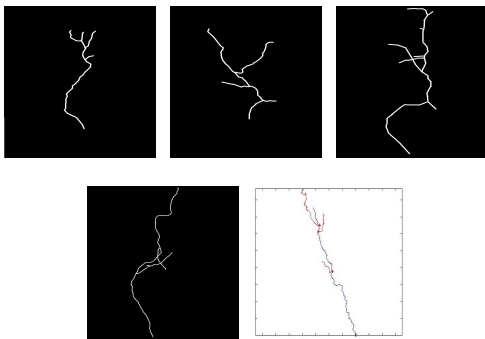
Validation



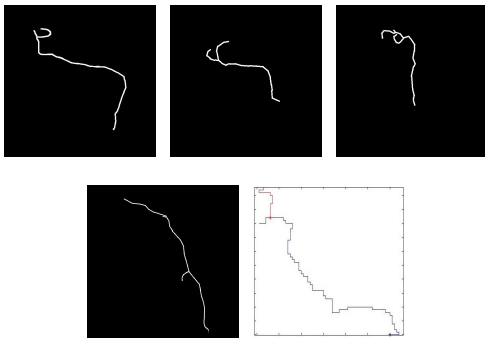
Results: Axon Simulation

- The parameters were estimated for each axon in the database and averaged between images of the same population to obtain representative values for each population
- Synthetic axons were generated and compared with real trees of each population

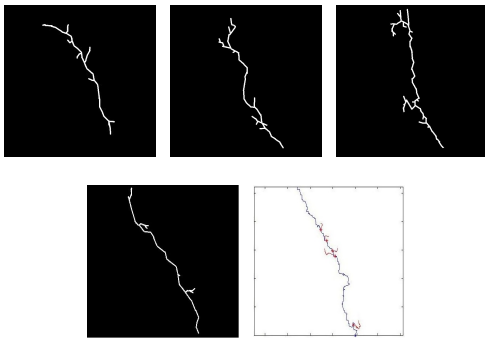
Results - Axon Simulation - Normal Tree



Results - Axon Simulation - Mutant Type 1 Tree

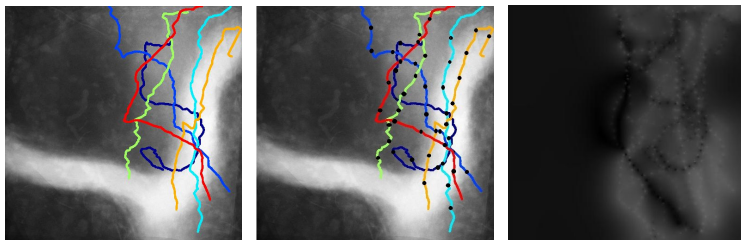


Results - Axon Simulation - Mutant Type 2 Tree



Results - Field Estimation

- We have calculated a scalar field (E_a/E_b) and a vector field (Δ) for each image
- Field extrapolation (using Gaussian Markov Random Field) to obtain non sparse fields (2 per population)
- Fields are plotted on the (registered) neuronal structure in which axons are developing (channel 2)



Results - Δ Field - Normal

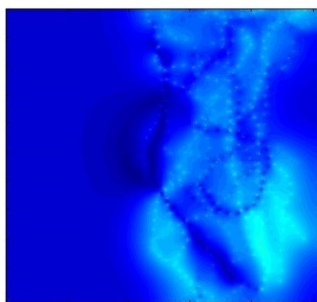
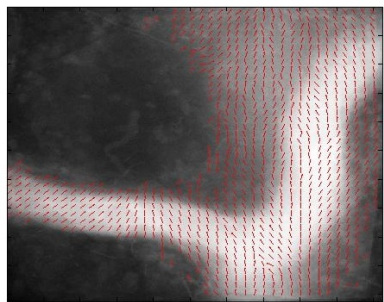


Figure: Direction (left) and norm (right) of the Δ field for the normal population.

Results - Δ Field

- Qualitative comparison between the Δ fields of different populations suggest no relevant difference between them
- Field points towards the target area (top right corner of the image)
- Field norm is stronger at the starting point of the axons (bottom right section) and weaker near the target area.

Results - E_a/E_b Scalar Fields

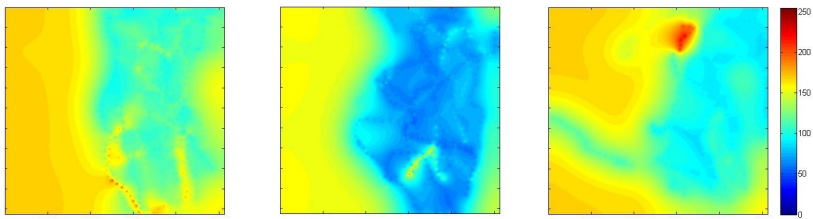


Figure: E_a/E_b scalar field for the normal (left), mutant type 1 (middle) and mutant type 2 (right) populations.

Results - E_a/E_b Scalar Fields

- Qualitative comparison between the fields of different populations
- Significant difference between the populations
- E_a/E_b is related to the flexibility of the axons, thus:
 - Normal axons have a more constant direction throughout their length, followed by mutant type 2 and mutant type 1

Summary

- 2D discrete stochastic model for the simulation of axonal biogenesis
- Several independent processes (elongation, shape and bifurcation) are considered
- Parameters estimated from real static data
- Validated on 53 images
- Generated synthetic axonal trees resemble real ones
- Parameters provide additional information on the populations
- **Limitations:**
 - Only 2D, real process in 4D
 - Requires more components to model all the necessary biological processes (retraction, competition, etc)

Outline

- 1 Introduction
- 2 Axon Extraction from Fluorescent Confocal Microscopy Images
- 3 Distance Between Trees Using the Elastic Shape Analysis Framework
- 4 Discrete Stochastic Model for the Generation of Axonal Trees
- 5 Conclusions

Conclusions

Conclusions

- We proposed a set of tools for the morphological analysis of axonal trees that covers the entire analysis process:
 - Segmentation algorithm for confocal microscopy images
 - Tree comparison method and computation of mean shape
 - Model for the generation of axonal trees
- Evaluation on a large database of images
- Different populations were considered

Future Work

- Segmentation:
 - Improve validation (full IBV database)
 - Automatic selection of the parameters
 - Integrate it in an easy-to-use open software (PIB platform)
- ESA Distance:
 - Analyze additional tree-like structures (blood vessels, airways)
 - Automatic selection of the parameters
 - Several unanswered mathematical questions (real metric, geodesics)
- Stochastic Model:
 - 3D / 4D extension
 - Validation of field
 - Validation of synthetic trees

Conclusions

Thanks

Thank you!